

Velocity Control of Linear Switched Reluctance Motor for Prototype Elevator Load

Abstract. In this study, a double-sided, 12/8 poled, 3 phased Linear Switched Reluctance Motor (LSRM) designed, manufactured and its velocity simulated by fuzzy logic control. Motor power is about 900 W. LSRM drive applied to a prototype elevator. LSRM motion distance is 2000 mm and it having about 500 N propulsion force used in locations such as elevators where linearly moving accurate position, easy control and rapid response are requested. Its operation and switching sections as motor and generator are determined and the simulation of fuzzy logic and PI speed and position control are simulated. Reference velocity is constant during the accelerating and decelerating. As a different, reference velocity is variable depended to position and time. The velocity of translator was controlled versus to position by Fuzzy Logic Control (FLC) and PI control techniques. Velocity and velocity error signals of translator separately were compared the simulation results PI and FLC techniques. It is concluded that the designed motor in the simulation according to the values determined values may be used in elevator as a driver.

Streszczenie. W pracy przedstawiono projektowanie, budowę oraz sterowanie z użyciem logiki rozmytej podwójnego, trójfazowego liniowego silnika reluktancyjnego przełączalnego (LSRM). Silnik LSRM zastosowano do budowy prototypu windy. Moc badanego silnika wynosiła około 900W, posiadał on zakres ruchu 2000 mmm i około 500 N siły napędowej. Ze względu na liniowy ruch, możliwość ustalenia dokładnej pozycji, prostego sterowania i możliwości szybkiego reagowania zaproponowano zastosowanie omawianego napędu w takich urządzeniach jak windy. Działanie napędu było realizowane zarówno w rzeczywistym prototypie, jaki i symulowane, z wykorzystaniem logiki rozmytej i regulatora PI kontrolującego prędkość i pozycję. Wyniki pomiarów porównano z wynikami symulacji. (Budowa oraz sterowanie z użyciem logiki rozmytej podwójnego, trójfazowego liniowego silnika reluktancyjnego przełączalnego)

Keywords: Linear SRM, LSRM and elevator, Longitudinal flux SRM, LSRM control, Fuzzy Logic Control

Słowa kluczowe: Liniowy SRM, LSRM i windy, strumień wzdłużny SRM, sterowanie LSRM, logika rozmyta

Introduction

Switched Reluctance Motors (SRM) have low production costs and easy design because of their simpler geometric structures compared to other electric motors. Their control systems and driver designs are easier in comparison to widely used induction motors. When the geometry of this motor is linearly designed, it is called as Linear Switched Reluctance Motor (LSRM). These motors are designed to be salient poled with different rotor and stator combinations. A LSRM has the same advantages as a SRM. However, it requires the usage of sensitive rotor position information and a special driver circuit. Moreover, the linear structure of LSRM enables it to be designed single-sided or double-sided with transverse or longitudinal flux [1-2]. Through the developing power electronic components and microcontrollers, an easy and flexible control strategy and a driver system, it is possible for LSRMs to be used in direct drive systems [2].

Despite the fact that there are many studies related to various rotary type SRMs and their control in literature, studies related to LSRM are quiet few. Nevertheless, it is possible to encounter some studies about design, simulation and control of LSRM for various applications.

In the Literature, the use of LSRMs for the primary propulsion of a ship elevator is proposed and investigated. A new type of LSRM is proposed with twin stators and a translator between them with no back iron in the translator

[3-4]. A SRM drive has been investigated and recommended as an alternative actuator for vertical linear transportation applications such as a linear elevator. A prototype home elevator with LSRMs is designed, and extensive experimental correlation is presented [3-4].

There are some studies for linear reluctance motor and linear synchronous reluctance motor in literature. The studies consist of LSRM and driver designs, simulations, FEA analysis, position and speed control strategies and applications in prototype elevator, elevator door, automatic door and railway vehicles [3-16].

Double Sided Linear Switched Reluctance Motor

In this study, LSRM is designed to be double-sided and its stator to be without yoke. Thus, a balanced and high power design with reduced cost and weight was obtained. LSRM consists of stator parts and twin translator sections. The translator is the section with windings and the section without windings is the stator. The moving section is describes as active. In this study, the LSRM has 3 phases, a 12 poled active translator, and an 8 poled passive stator without yoke. The number of stator poles is dependent on the length of the linear mobility system. As herein implied, the 8 stator poles are the ones which are located between the double sides of the motor, are included in magnetic coupling and enable the motion [2].

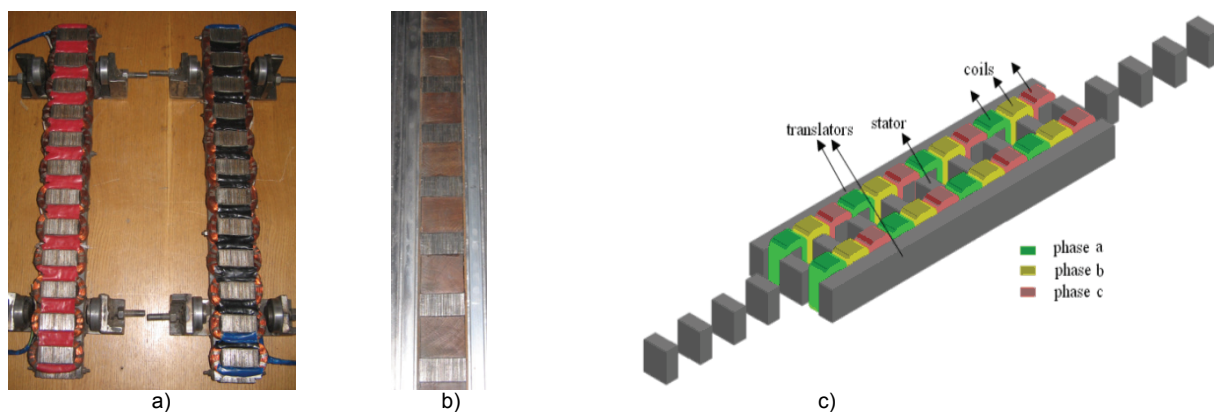


Fig.1 Double sided LSRM [2] a) twin translator b) stator c) simulator model

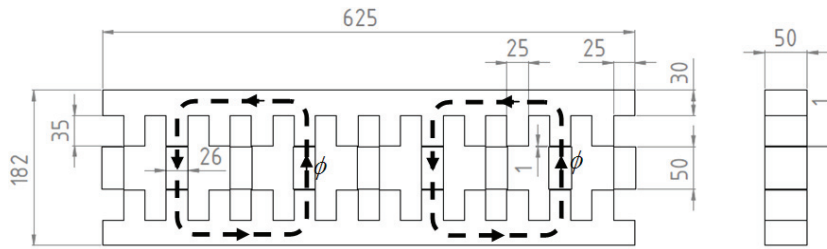


Fig.2. Sizes of LSRM [2]

The size variables and application model of the double-sided LSRM are given in Fig. 1, the sizes and flux paths are presented in Fig. 2 [2]. For each phase, there are 4 conjugate pairs and a total of 8 windings. Windings belonging to the same phase are serially connected. Therefore, by decreasing the input current of each phase, the cost for semi-conductor switching components was reduced [2].

Proposed LSRM is analyzed by using 3D FEM. A phase coils of the motor is excited 2000 and 3000 At magneto motive force (mmf). Simulation results are obtained according to phase current and rotor positions for phase inductance. Phase inductance results obtained by the simulations, analytical calculations and measurements are presented in Fig. 3 [2].

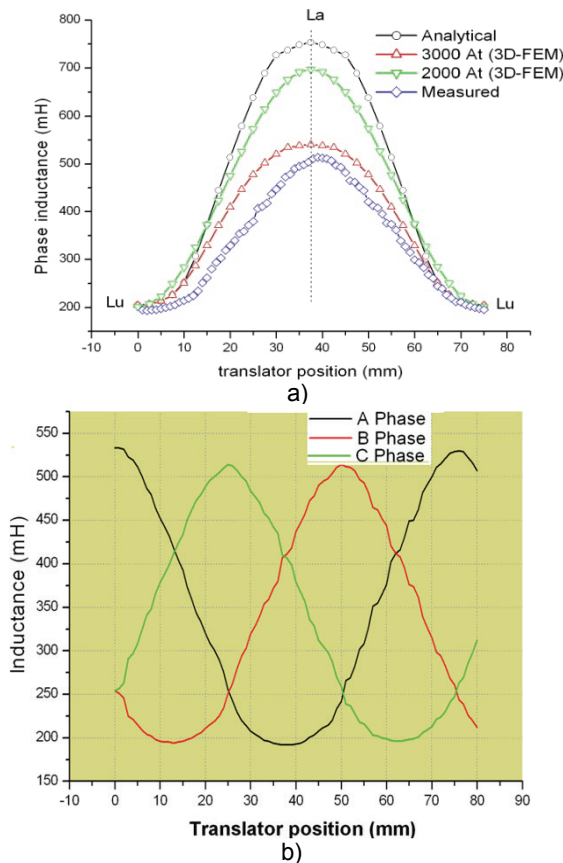


Fig. 3 Phase inductance profile of LSRM [2] a) A phase inductance, b) measured 3 phase inductance

Double sided LSRM is generated forces at 3 axes which are propulsion (F_x), drag (F_y) and lateral (F_z) forces. Directions of the forces are given in Fig. 4. Resultant drag force is zero because F_y forces are balanced by counter poles. Forces component are calculated by Eq.1. F_x provides the linear movement and the velocity of the LSRM.

$$(1) F_x = \frac{B_g^2}{2\mu_0} YZ = \frac{B_g^2}{2\mu_0} l_{sl} l_g, F_y = \frac{B_g^2}{2\mu_0} XZ = \frac{B_g^2}{2\mu_0} l_{sl} l_{tp}$$

where B_g is magnetic flux density in airgap, pole dimensions, l_{sl} , l_g and l_{tp} are shown in Fig.4.

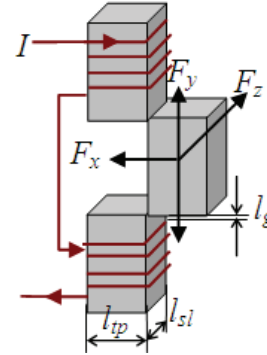


Fig.4. Force components and directions

Mechanical Prototype Elevator Design

The prototype elevator system was driven by LSRM. Moving part active translator moves the cabinet directly. Weight of cabinet and translator is about 40 kg and it balanced counter weight over the rope. Mechanical brake which operate electromagnetically block the rope and so cabinet is braked. Moreover motor can brake the cabinet magnetically in LSRM aligned position. Cabinet position data is obtained from linear encoder which is mounted the elevator. Cabinet can be stopped any location according to position data. Therefore it needn't sensors or limit switches for all locations because linear encoder generate position data each 62.5 μ m. Prototype elevator system is shown in Fig.5 and Fig.6.

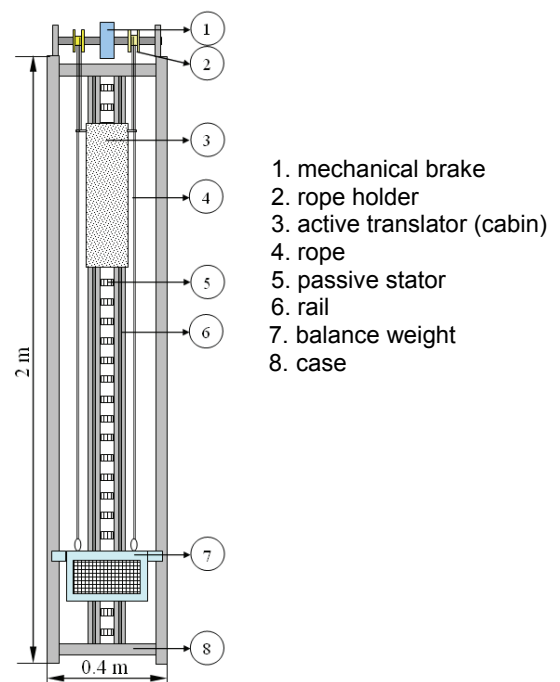


Fig. 5. Prototype elevator parts

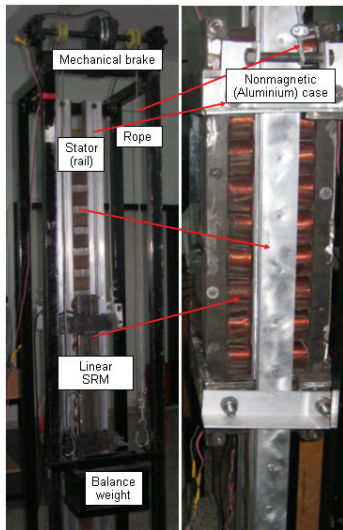


Fig. 6. Prototype of elevator driven by double sided LSRM

Driver system

In order to feed LSRM, many converter structures has been suggested and studied in the literature. The H bridge converter is used for prototype elevator driven by LSRM Figure 7 shows the block diagram of LSRM control circuit.

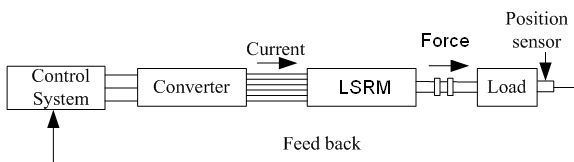


Fig.7. Block diagram of the LSRM control circuit

DC source feeds the motor power layer. For each phase of the 3 phased power layer, 2 IGBTs are used in converter. Rotor position is sensed through counting the pulses obtained from the magnetic and contactless linear position sensor. It produces pulses at each 62.5 μm. A phase switching period is 25 mm which it is distance between overlap and aligned positions of LSRM. Elevator cabin is moved 75 mm after 3 phases excited in a cycle. PWM outputs of microcontroller provide the switching in a phase excitation. Block diagram of the control system is presented in Fig. 8.

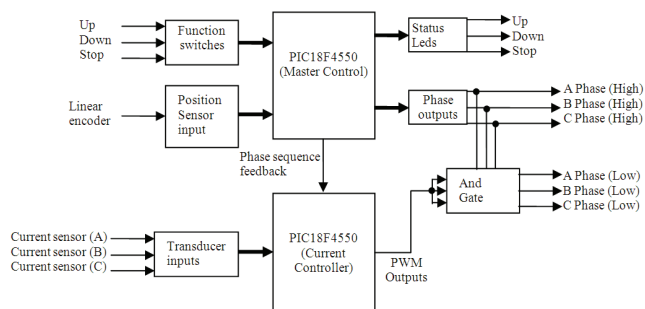


Fig.8. Control system's block diagram of prototype elevator

Driver system consist of H bridge converter, IGBT modules and drivers, snubber capacitors, feedback diodes, current transducers, linear position sensor, PIC master control module and feeding layer. Driver system is protected for over load in order to protect IGBTs. Current is measured by current sensors. If each phase reaches the current limit

microcontroller operate in safety mode. In this mode PWM output is zero.

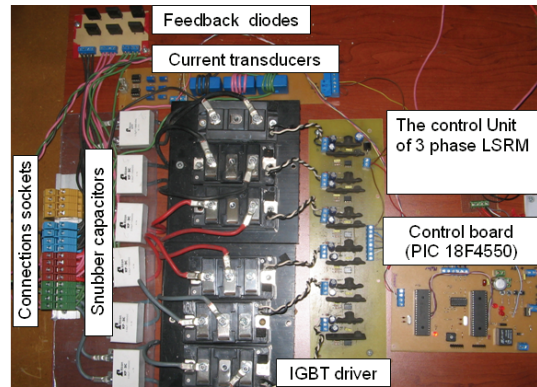


Fig.9. Driver system

Elevator control algorithm is given in Fig.10.

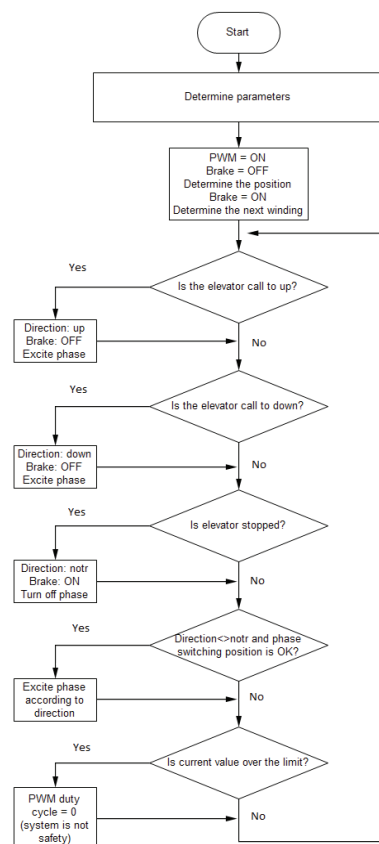


Fig.10. Elevator control algorithm flowchart

LSRM velocity control with fuzzy logic method

Fuzzy logic controller will be used to control the velocity of LSRM. The input variables of the system in the fuzzy logic controller will be defined as (e) velocity error and (ce) the change in the velocity error. The error and the change in error obtained are converted into per unit value. The triangle membership function curves that will be used to calculate the membership values of these values are shown in Fig.11. It shows membership values of the fuzzy logic. Fig. 12 shows the design of a fuzzy logic controller system. Fig. 13 shows block diagram of the fuzzy logic controller system [7-9,16].

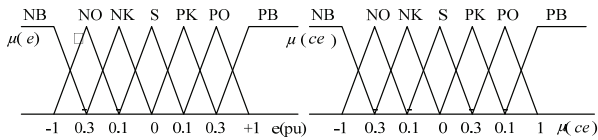


Fig. 11. Membership values of the fuzzy logic

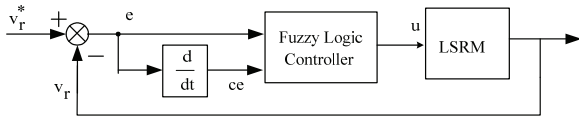


Fig. 12. Fuzzy logic controller system

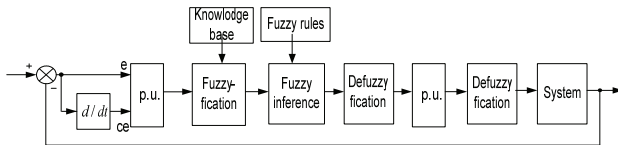


Fig.13. Block diagram design of a fuzzy logic controller system.

The output of the fuzzy logic is the reference current value of the motor. The velocity of the motor has controlled by this way. The input variables of the system follow as

$$(2) \quad \begin{aligned} e_{v_r}(k) &= v_r^*(k) - v_r(k) \\ ce_{v_r}(k) &= e_{v_r}(k) - e_{v_r}(k-1) \end{aligned}$$

where, $v_r^*(k)$ is the reference velocity at k^{th} sampling moment, $ce_{v_r}(k)$ is the change in velocity error at k^{th} sampling moment. The input variables transferred into the unit value (pu) is defined as;

$$(3) \quad \begin{aligned} e(pu) &= e_{v_r}(k) / GE \\ ce(pu) &= ce_{v_r}(k) / GC \end{aligned}$$

The output definition of the fuzzy logic controller is

$$(4) \quad I_K = I_{(K-1)} + GU * du(pu) \quad \square$$

where, I_K is the controller output value for the k^{th} sampling, $I_{(K-1)}$, is the previous controller output value of the k^{th} sampling and $GU*du(pu)$ is the output reaction for the k^{th} sampling. GE is constant of per unit rate for error, GU is constant of per unit rate for changing of error and GU is constant of rate for defuzzification. The obtained value of is the reference current which controls the velocity of LSRM.

Simulation Results

In the simulation the velocity of LSRM is controlled by velocity feedback and fuzzy logic and PI control methods.

Fig. 14 shows phases currents at 150 N load with PI controlled LSRM. Fig. 15 shows velocity changing at 400 N load with PI controlled LSRM. Figure 16 shows velocity error at 400 N load with PI controlled LSRM. Fig. 17 shows phases currents at 400 N load with PI controlled LSRM. Fig.18 shows velocity changing at 500 N load with PI controlled LSRM. Fig. 19 shows velocity error at 500 N load with PI controlled LSRM. Fig.20 shows phases currents at 400 N load with FLC controlled LSRM. Fig.21 shows velocity of FLC controlled LSRM. Fig.22 shows velocity error at 400 N load with FLC controlled LSRM. Fig.23 shows velocity changing at 400 N load with FLC controlled

LSRM. Fig. 24 shows velocity error at 400 N load with FLC controlled LSRM.

The LSRM used for simulation is with 3 phases, 12/8 poles, 8 A, 85 V, 900 W, 2.5 m/s nominal velocity, $B=0.03$ coefficient of friction, $J=0.0067 \text{ kgm}^2$ momentum of inertia. The source voltage is 85 V and the output of converter is stable.

Switching zones of phase currents and strategies are determined according to translator position of the motor from the inductance curves. Maximum current values is limited 8 A. In this simulation motor is not fully loaded.

With the purpose of monitoring the response of the designed linear motor against the rotational one, its velocity is controlled and oscillations in the velocity are found by using PI control method. When k_i is taken 1 and k_p 62 in the control, velocity alteration of PI controlled LSRM under a fixed load is seen in Fig. 15. As seen here, the motor has reached the nominal velocity in a distance of about 20 mm and velocity response of PI controlled LSRM. Linear velocity alteration of PI controlled LSRM having the same parameters are given in Fig.14 to Fig.17. It is observed that the motor has reached 2.5 m/s velocity in 20 mm. Fig. 14 the velocity of translator of LSRM is applied to elevator directly.

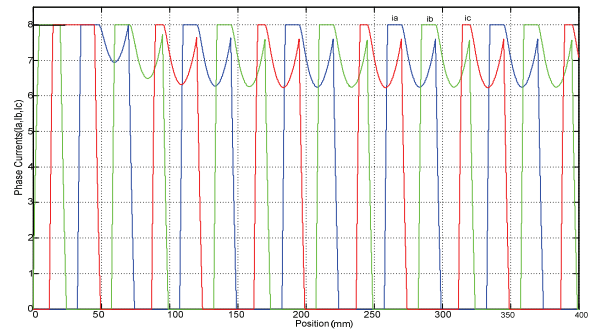


Fig. 14. Phases currents at 150 N load with PI controlled LSRM

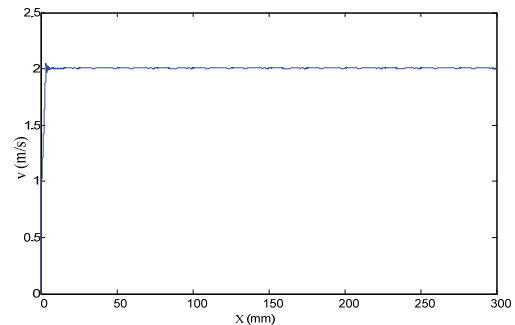


Fig. 15. Velocity changing at 400 N load with PI controlled LSRM

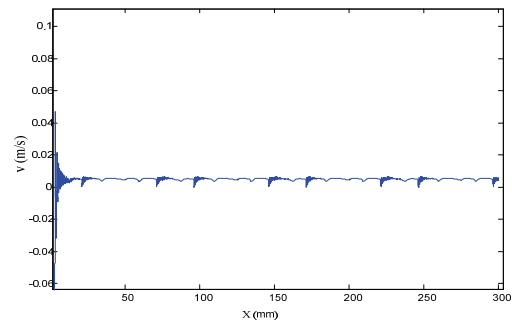


Fig. 16. Velocity error at 400 N load with PI controlled LSRM

With the purpose of monitoring the response of the designed linear motor its velocity is controlled by using PI control method. If it takes as k_i 5 and k_p 55 in the control, velocity of PI controlled LSRM under a fixed load is seen in Fig. 18. As seen here, the translator has reached the nominal speed in a distance of about 20 mm. But, in this control scheme velocity is not stable. As seen in Fig.19 velocity error under 500 N load there are about 0.3 m/s velocity error periodically.

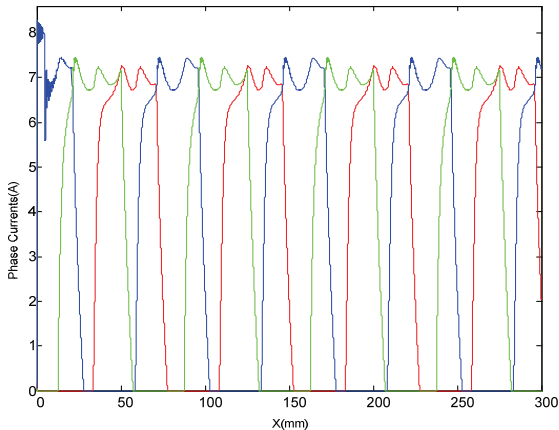


Fig. 17. Phases currents at 400 N load with PI controlled LSRM

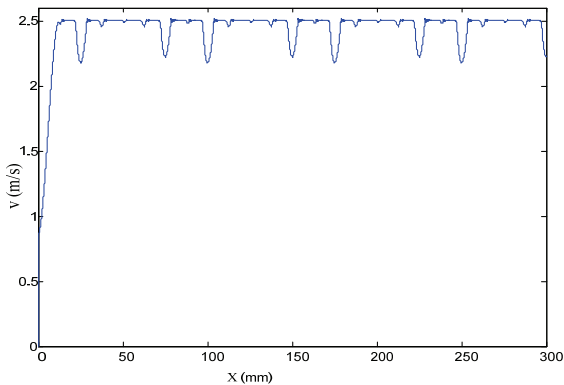


Fig.18. Velocity changing at 500 N load with PI controlled LSRM

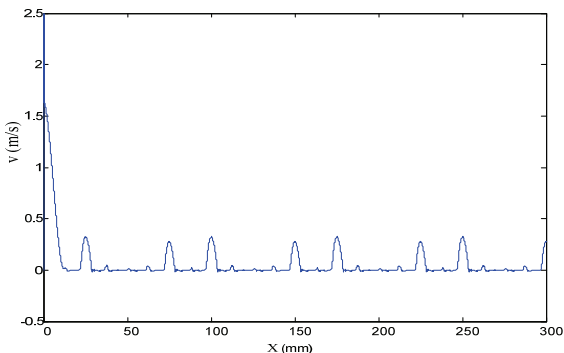


Fig. 19. Velocity error at 500 N load with PI controlled LSRM

LSRM having the same parameters by FLC method are given in Fig.20 to Fig.24. It is observed that the motor has reached 2.5 m/s speed again at 20 mm. In Fig.20 phases currents under 400 N load by FLC control. As seen that phases currents signals are more smoothly by FLC control method than PI control method. As seen that in Fig.21 linear speed changes of FLC controlled LSRM smoothly than PI control method. Moreover, as seen that in Fig.22 velocity error is small than PI control method.

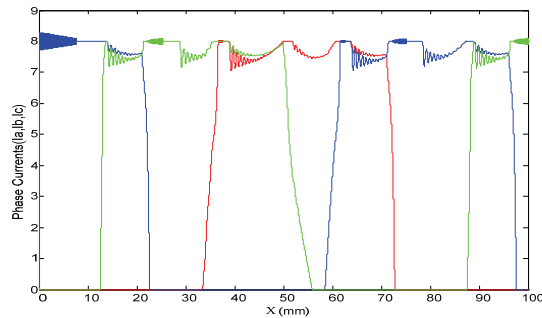


Fig.20. Phases currents at 400 N load with FLC controlled LSRM

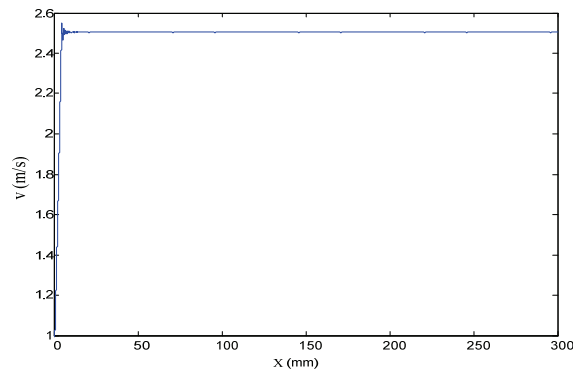


Fig.21. Velocity of FLC controlled LSRM

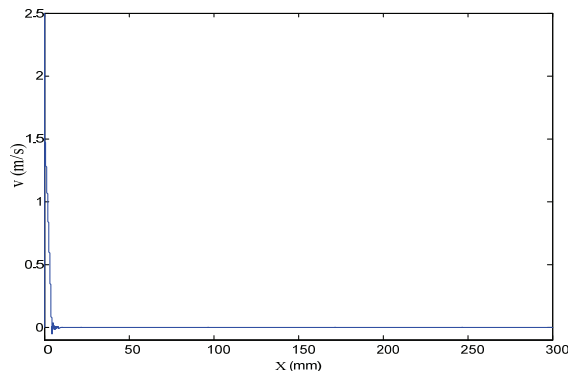


Fig.22. Velocity error at 400 N load with FLC controlled LSRM

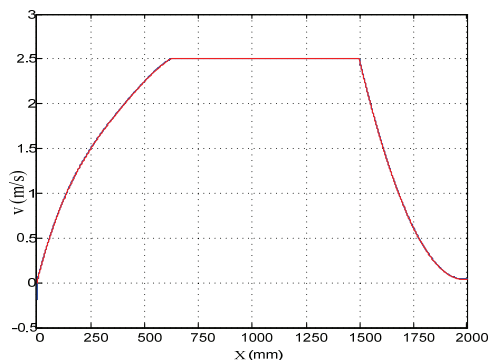


Fig.23. Velocity changing at 400 N load with FLC controlled LSRM

In Fig.23 reference velocity is not constant to get resembled elevator cabinet velocity during the accelerating and decelerating. So, it has been tested velocity of translator versus to position. It can be seen that from this figure, response of translator velocity is sufficient to cabinet carry. The velocity error is acceptable in Fig.24. It was given Phase A current at variable velocity in Fig.25. Variable reference velocity equations were given Eq.5 to Eq. 8.

- (5) if($0 \leq X < 625$) $\{v_1 = -667.5 \cdot 10^{-15} \cdot X^5 - 303030 \cdot 10^{-15} \cdot X^4 + 39015 \cdot 10^{-11} \cdot X^3 - 12320 \cdot 10^{-8} \cdot X^2 + 23357.5 \cdot 10^{-6} \cdot X - 21.6458\}$ $\{v_2 = 0.0; v_3 = 0.0\}$
- (6) if($X \geq 625$ and $X < 1500$) $\{v_1 = 0.0; v_2 = 2.5; v_3 = 0.0\}$
- (7) if($1500 \leq X \leq 2000$) $\{v_3 = 65 \cdot 10^{-6} \cdot X^2 - 10315 \cdot 10^{-5} \cdot X + 49.96\}$ $\{v_1 = 0.0; v_2 = 0;\}$
- (8) $V_{ref} = V_1 + V_2 + V_3$ (m/s)

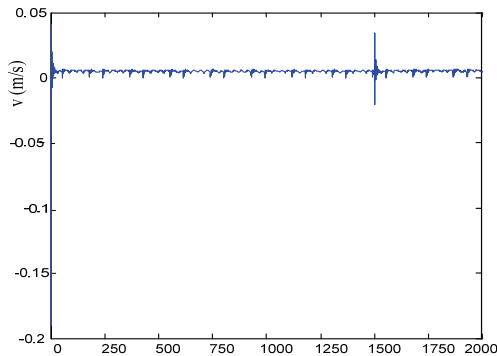


Fig. 24. Velocity error at 400 N load with FLC controlled LSRM

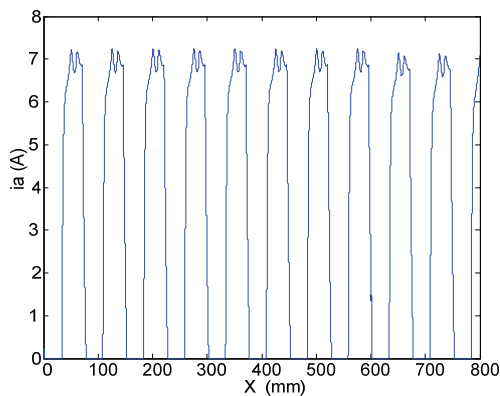


Fig. 25. A Phase current at 400 N load FLC controlled LSRM

Conclusion

In this study, the response of fuzzy logic velocity controlled double sided LSRM which have 12/8 poled, 3 phase, 85V, 900 W power is simulated and than PI and fuzzy logic velocity responses of the motor is compared. Since in this system friction is reduced because there is not any brush and collector in the motor and the motor efficiency is high. In addition, the losses arising from gear box power transfer are prevented and cost is reduced by removing the power transfer elements used in excess.

As a result, it is concluded that the motor may be used in places such as elevator load. The other side the accurate position control, high starting force and rapid response are requested because of their low cost, high efficiency and high rate force/volume.

Acknowledgement

This study has been supported by Gaziosmanpasa Uni. Scientific Research Projects Commission. It is extended and revised version of presented paper (143) in SMC2011.

REFERENCES

- [1] Krishnan, R.: Switched Reluctance Motor Drives, Washington, D.C: CRC Pres, (2001), Chapter 3.
- [2] Fenercioglu A., Dursun M., Design and magnetic analysis of a double sided linear switched reluctance motor, Przeglad Elektrotechniczny, 86 (2010), No. 5, 78-82.
- [3] Lim, H.S., Krishnan, R., Lobo, N.S.: Design and Control of a Linear Propulsion System for an Elevator Using Linear Switched Reluctance Motor Drives, IEEE Transactions On Industrial Electronics, 55 (2008), No. 2, 1584-1591.
- [4] Lim H.S, Krishnan R., Ropeless Elevator With Linear Switched Reluctance Motor Drive Actuation Systems, IEEE Transactions On Industrial Electronics, 54 (2007), 2209-2218.
- [5] Dursun M., Koc F., Ozbay H., Determination of Geometric Dimensions of a Double Sided Linear Switched Reluctance Motor, (2010), 282-238, Paris, France.
- [6] Dursun M., Koc F., Ozbay H., Ozden S., Design of Linear Switched Reluctance Motor Driver For Automatic Door Application, International Conference on Information and Industrial Electronics (ICIIE), (2011), 424-427, China.
- [7] Dursun M., Koç F., Simulation of Fuzzy Logic Position and Speed Control of Double Sided Linear Switched Reluctance Motor, ICMSC International Conference on Modeling, Simulation and Control, (2010), 517-521, Egypt.
- [8] Dursun, M., Özden, S., Simulation and application of fuzzy logic controlled adjustable speed switched reluctance motor to elevator system, Journal of Polytechnic, 11 (2008), No.2, 129-137
- [9] Dursun M., A wheelchair with fuzzy logic controlled switched reluctance motor supplied by PV arrays, Journal of Applied Sciences, 8 (2008), No.19, 3351-3360
- [10] Kjaer, P.C., Gribble, J.J., and Miller, T.J.E., High-grade control of switched reluctance machines, IEEE Trans. Ind. Electronics, 33 (1997), No.1585-1593
- [11] Boldea, I and Nasar, S.A, Linear Electric Actuators and Generators, Cambridge, U.K.: Camb. Univ. Press, (1997).
- [12] Bae H. K., Lee B. S., Vijayraghavan P., and Krishnan R., A linear switched reluctance motor: converter and control, IEEE Trans. Ind. Appl., 36 (2000), 1351-1359.
- [13] Lim HS and et al., Design and Control of a Linear Propulsion System For An Elevator Using Linear Switched Reluctance Motor Drives, IEEE Trans. On Ind. Electronics., 55 (2008), No.2, 534-542
- [14] Kolomeitsev L., Kraynov D., Pakhomin S., Rednov F., Kallenbach, E., Kireev, V., Schneider, T., Böcker, J., Linear Switched Reluctance Motor as a High Efficiency Propulsion System for Railway Vehicles, SPEEDAM International Symposium on Power Electronics, Electrical, (2008), 155-160, Ischia.
- [15] Dursun M., Özbay H., Design And Analysis Of A Double Sided Linear Switched Reluctance Motor Driver For Elevator Door, Przeglad Elektrotechniczny, 5 (2011), 293-296.
- [16] Dursun M., Koc F., Simulation of Velocity Control of Linear Switched Reluctance Motor, 3rd International Conference on Computer Engineering and Technology (ICCET 2111), (2011), No:6, 236-242, 16-19 June, Kuala Lumpur, Malaysia

Authors:

Assoc. Prof. Dr. Mahir Dursun, Gazi University, Department of Electric Education, Faculty of Technology, 06500, Teknikokullar, Ankara, Turkey, e-mail: mdursun@gazi.edu.tr

Assist. Prof. Dr. Ahmet Fenercioglu, Gaziosmanpasa University, Department of Mechatronics Engineering, Faculty of Engineering and Natural Science, 60250, Taşlıçiftlik, Tokat, Turkey, e-mail: ahmet.fenercioglu@gop.edu.tr